Miscible Blends of Two Crystalline Polymers. 2. Crystallization Kinetics and Morphology in Blends of Poly(vinylidene fluoride) and Poly(1,4-butylene adipate)

J. P. Penning[†] and R. St. John Manley*

Department of Chemistry, McGill University, 3420 University Street, Montreal, Quebec H3A 2A7, Canada

Received May 15, 1995; Revised Manuscript Received September 29, 1995[⊗]

ABSTRACT: The crystallization kinetics and morphology in miscible blends of poly(vinylidene fluoride) (PVF_2) and poly(1,4-butylene adipate) (PBA) have been investigated using optical microscopy and differential scanning calorimetry. Blends of PVF_2 and PBA are unique in the sense that both components are capable of crystallization over a wide range of compositions. The kinetics of crystallization of both PVF_2 and PBA in these blends have been investigated. During the crystallization of the high-T_m component (PVF_2, $T_m \approx 175$ °C), the low-T_m component (PBA, $T_m \approx 60$ °C) acts as a noncrystalline diluent. Addition of PBA depresses the radial spherulitic growth rate and overall crystallization rate of PVF_2 and affects the texture of PVF_2 spherulites but does not significantly alter the nature of the nucleation and growth processes of this polymer. During the crystallization of PBA, the PVF_2 phase is always partially solidified and the presence of the spherulitic microstructure of PVF_2 profoundly influences the crystallization behavior and morphology of PBA. The overall crystallization rate of PBA goes through a maximum as a function of PVF_2 content, which is explained in terms of the combined effects of enhanced heterogeneous nucleation and reduced linear growth rate. The mechanism of crystal growth is modified in the presence of PVF_2, as indicated by a change in the Avrami exponent. In the blends, spherulitic crystallization of PBA is not observed, in contrast to the bulk crystallization behavior of this polymer. Crystallization of PBA from the blends initially takes place at the boundaries of PVF_2 spherulites, but at longer crystallization times, crystallization of PBA within PVF_2 spherulites is also observed. The observed phenomena are unique to blends of two crystalline polymers.

Introduction

The miscibility and phase behavior of binary polymer blends has been a subject of continuing interest for researchers from both scientific and industrial fields. Among the great variety of polymeric mixtures, those involving semicrystalline polymers are particularly interesting. This is not only because semicrystalline polymers are of prime importance from the commercial point of view but also because semicrystalline polymer blends offer the possibility of studying crystallization and crystalline morphologies in relation to miscibility in high polymers. Studies of this kind have been mainly focused on blend systems containing one semicrystalline polymer.[1−6] Blends in which both components are semicrystalline polymers, on the other hand, are more complicated and thus open up new avenues for studying the relations between phase behavior and structure development in polymeric mixtures. Of particular interest is the formation and morphology of the semicrystalline/semicrystalline state since it involves the crystallization of two different polymers, each within its specific temperature regime. The study of the crystallization kinetics in these blend systems is therefore not only concerned with the effects of blend composition and crystallization temperature but also addresses the question of how the crystallinity of the one component affects the crystallization behavior of the other. So far, these issues have not been given much attention, except for a recent series of papers by Stein and co-workers on blends of polycarbonate and polycaprolactone.[7−10]

In a recent paper,[11] we have described the miscibility and phase behavior of mixtures of poly(vinylidene fluoride) (PVF_2) and poly(1,4-butylene adipate) (PBA), a blend system in which both constituents are semicrystalline polymers. Mixtures of PVF_2 and PBA exhibit a complicated phase behavior and undergo multiple phase transitions. On the basis of the observation of a melting point depression and a single glass transition temperature, it was concluded that PVF_2 and PBA are thermodynamically miscible in the melt. Over a wide range of compositions, both PVF_2 and PBA readily crystallize from the mixtures, which leads to the formation of very rich and intriguing morphologies. At room temperature, the blends exhibit a three-phase morphology in which two different crystalline phases co-exist with an intimately mixed amorphous phase.

In the present work, we have undertaken an investigation into the crystallization behavior and morphology in semicrystalline/semicrystalline blends of PVF_2 and PBA. The phase diagram of the PVF_2/PBA system exhibits two distinct melting transitions, one for the PBA component, located around 60 °C, and one for the PVF_2 component at about 175 °C. Above the melting point of PVF_2, the blends form a homogeneous, single-phase melt. Lowering the temperature to $T < T_m(PVF_2)$ results in the crystallization of the PVF_2 component, which amounts to the transition from the fully amorphous to the amorphous/semicrystalline state. When the temperature is further lowered to $T < T_m(PBA)$, the PBA component crystallizes as well, bringing the system from the amorphous/semicrystalline into the semicrystalline/semicrystalline state. We have investigated the kinetics of both of the above-mentioned phase transitions through measurement of the overall crystallization rates as well as radial spherulitic growth rates. In addition, the morphologies of the blends, at various points in the phase diagram, have been examined by means of optical microscopy.

* To whom correspondence should be addressed.
[†] Present address: Akzo-Nobel Central Research, Department RDS, P. O. Box 6300, 6800 SB Arnhem, The Netherlands.
[⊗] Abstract published in *Advance ACS Abstracts,* November 15, 1995.

0024-9297/96/2229-0084$12.00/0

Experimental Section

The general procedures of blend preparation and characterization of thermal behavior by means of differential scanning calorimetry are described in detail in a previous publication.[11] The blend compositions are indicated in ratios of weight percent, the first numeral referring to PVF_2 throughout this paper. Isothermal crystallization experiments were conducted with approximately 2−5 mg samples which were premelted at 200 °C for 10 min prior to each experiment. The samples were then quenched to the appropriate crystallization temperature at a rate of 200 °C/min. In the case of isothermal crystallization of PBA from the blends, the samples were annealed at 100 °C for 1 h in order to allow full crystallization of the PVF_2 component prior to the actual crystallization experiment. The melting points and heats of fusion of the crystallized samples were measured at a scanning rate of 5 °C/min.

Samples for optical microscopy were prepared by filtering a solution of the blend in *N*,*N*-dimethylformamide onto a clean glass cover slip and drying in vacuum at room temperature for 3 days. The resultant films were approximately 5 μm in thickness. Photomicrographs were obtained using a Nikon Microphot FXA polarizing microscope equipped with a Mettler FP82 hot-stage and a Nikon FX-35DX camera. Measurements of spherulitic growth rates were performed using a Nikon Optiphot polarizing microscope equipped with a Linkam THMS 600 hot-stage. The samples were preheated at 200 °C for 5 min and quenched to the desired crystallization temperature at a cooling rate of 130 °C/min. Spherulitic growth was monitored under crossed polars using a video camera mounted on the microscope. The images were recorded on videotape and the JAVA (Jandel Scientific) image analysis software was used to determine the spherulite sizes at various crystallization times. Growth rates were obtained from linear regression of the spherulite radius as a function of time, which usually yielded a correlation coefficient of 0.999 or better.

Wide angle X-ray scattering patterns of various blends were recorded with a flat-film camera with the use of nickel-filtered Cu Kα radiation, produced by a Philips X-ray generator operating at 40 kV and 20 mA. The samples used in these experiments were prepared by compression molding and consisted of films of approximately 0.5 mm in thickness. Calibration of the sample-to-detector distance was performed using NaF powder.

Results and Discussion

Phase Behavior. In order to facilitate the understanding of the crystallization kinetics in PVF_2/PBA blends, we have summarized the thermal behavior of these blends,[11] as determined by means of differential scanning calorimetry (DSC), in Figure 1. The melting points reported here refer to the equilibrium melting points that were obtained from Hoffman−Weeks analysis. The glass transition temperatures (T_g) were determined at a heating rate of 20 °C/min from the midpoint of the change in heat capacity. The "crystallization temperature" T_{max} corresponds to the maximum of the crystallization exotherm that is observed in the DSC trace when the blends are cooled from the melt at a cooling rate of 20 °C/min. From the T_{max} curves, it is evident that both PVF_2 and PBA readily crystallize from the mixtures over a wide range of compositions (80/20−20/80). Crystallization of PVF_2 takes place at temperatures well above the melting point of PBA, which means that the two polymers crystallize in well-separated temperature regimes and that the PVF_2 component will always be partially solidified before crystallization of PBA commences. It should be mentioned that due to the wide separation of crystallization regimes, as well as the large differences in the unit cell parameters of PVF_2 and PBA, cocrystallization is not expected to occur between the two polymers. The crystallization of each of the two blend components thus represents a phase separation process in which the polymers partially segregate from the mixture to form a pure phase. As indicated in the phase diagram in Figure 1, the blends can be classified as either completely amorphous (I), amorphous/semicrystalline (II), or semicrystalline/semicrystalline (III), depending on temperature and composition.

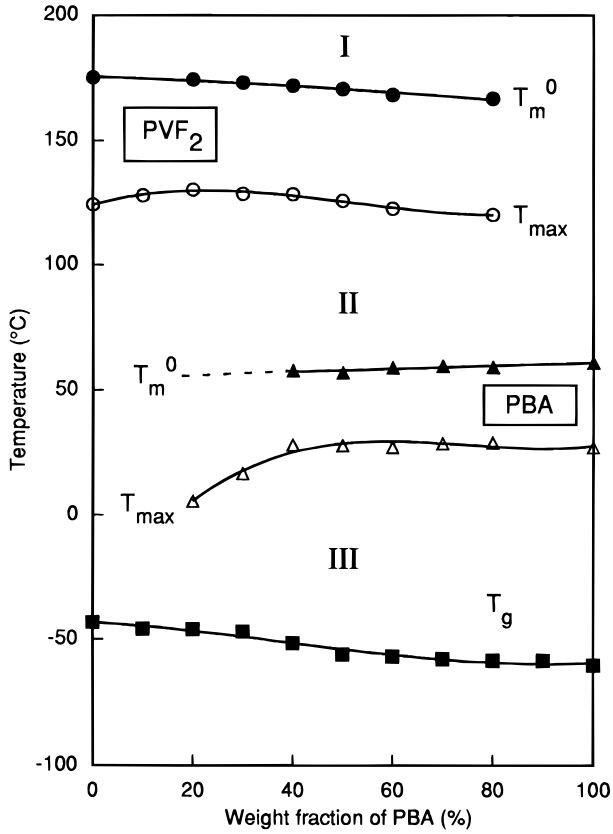

Figure 1. Phase diagram of the PVF_2/PBA blend system, showing the equilibrium melting points (T_m^0) and the crystallization temperatures (T_{max}) of both PVF_2 and PBA, as well as a single glass transition temperature (T_g).

Spherulitic Morphologies. The crystallization of PVF_2, which amounts to the transition from the fully amorphous to the amorphous/semicrystalline state, proceeds through free growth of spherulites from the homogeneous melt. Figure 2 shows the spherulitic morphology of the PVF_2 phase, at various blend compositions, after complete crystallization from the melt at 150 °C. The spherulites show the familiar maltese cross birefringent pattern and exhibit concentric extinction bands. In the 100/0 and 80/20 blends, these extinction bands are very tightly spaced and are not resolved at the current magnification. However, with increasing PBA content, the band spacing *S* becomes progressively larger and the banded textures are quite distinct in both 60/40 and 40/60 blends. Banded structures are commonly observed in polymeric spherulites and are believed to arise from cooperative twisting of radiating lamellar crystals about their axis of fastest growth.[12] It is usually found that *S* increases with crystallization temperature but decreases upon addition of noncrystallizing diluents.[12,13] Thus, the observed increase in *S* with PBA concentration is contrary to common finding. The reason for this is not entirely clear. It appears that, in the case of PVF_2/PBA blends, the band spacing *S* is related directly to the spherulitic growth rate: under all experimental conditions, *S*

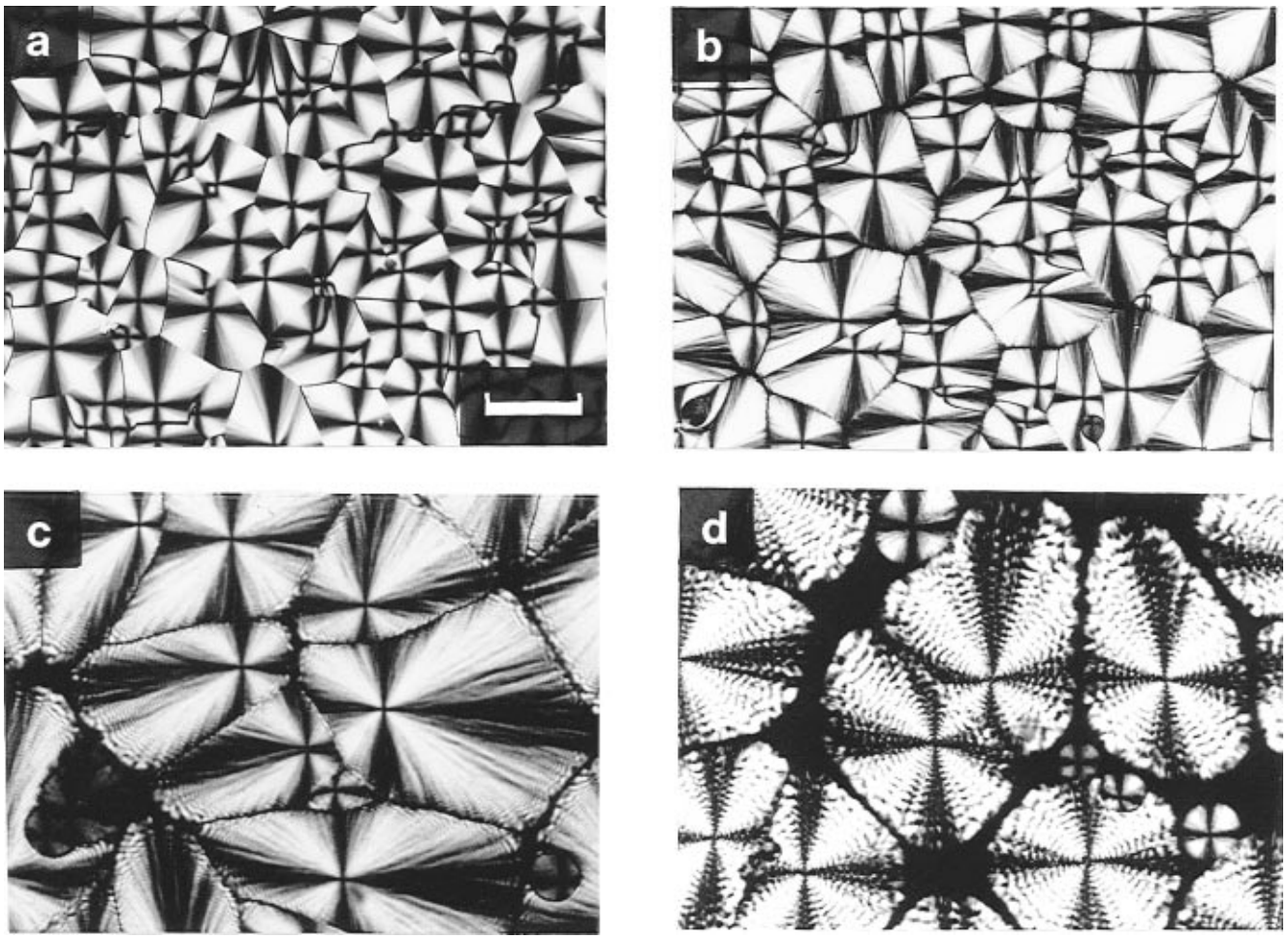

Figure 2. Optical micrographs (same magnification, bar = 50 μm) of the spherulitic morphology of PVF_2 in various blends with PBA after complete crystallization at 150 °C; (a) pure PVF_2; (b) 80/20, (c) 60/40, and (d) 40/60 PVF_2/PBA.

increases with decreasing crystal growth rate, i.e., with crystallization temperature and with increasing concentration of noncrystallizing component.

It is observed in Figure 2 that the spherulites become progressively larger with increasing PBA concentration, indicative of a decrease in nucleation density due to blending. Up to high PBA contents, the PVF_2 spherulites remain more or less space-filling, although nonbirefringent regions develop at the spherulitic boundaries in PBA-rich blends. The fact that the PVF_2 phase is more or less space-filling even at high PBA content indicates that the noncrystallizable PBA component, which is rejected in the crystallization process,[14,15] resides primarily in the interfibrillar domains of the PVF_2 spherulites.

The highly birefringent spherulites observed in pure PVF_2 correspond to the α-modification, which is the normal mode of crystallization for this polymer when crystallized from the melt at temperatures below 160 °C.[16] In the PBA-rich blends, spherulites of a second form are observed, which are smaller, exhibit lower birefringence, and appear to be more compact. These smaller spherulites have been observed frequently in PVF_2 crystallized at high temperatures (>160 °C) and are generally believed to correspond to the γ-modification.[16−18] Wide angle X-ray scattering (WAXS) experiments performed on a 50/50 blend that was crystallized at 150 °C revealed a reflection corresponding to $d = 3.98$ Å. This reflection was not observed for pure PVF_2 crystallized under the same conditions. The reflection at $d = 3.98$ Å is unique to the γ-form unit cell (111)[19] and this result therefore indicates the presence of the γ-polymorph in the blended state. The occurrence of the γ-modification at crystallization temperatures below 160 °C suggests that blending favors crystallization with this unit cell. A similar phenomenon has been observed in blends of PVF_2 with poly(methyl methacrylate).[5,20,21] This effect may be due to molecular interactions of PVF_2 with the PBA "solvent". It is well-known that PVF_2 favors the γ-form when crystallized from certain solvents.[17]

When the blends are cooled from the amorphous/semicrystalline state to a temperature below the melting point of PBA, this component will also crystallize and bring the system into the semicrystalline/semicrystalline state. This process is illustrated for a 40/60 blend in Figure 3 in a series of optical micrographs. The micrographs were obtained under crossed polars with the use of a 530 nm retardation plate and are reproduced here in color in order to emphasize the observed phenomena. Figure 3a represents the amorphous/semicrystalline state at 150 °C and shows the spherulitic morphology of the PVF_2 phase after complete crystallization at this temperature (cf. Figure 2d). Parts b and c of Figure 3 represent a time sequence of the crystallization of the PBA component that was induced by cooling the sample from 150 to 40 °C. It is seen that the crystallization of PBA commences in the interspherulitic domains of the pre-existing PVF_2 morphology and continues to take place in these interspherulitic regions, up to the point where they are more or less filled with PBA crystallites. After longer times, crystal-

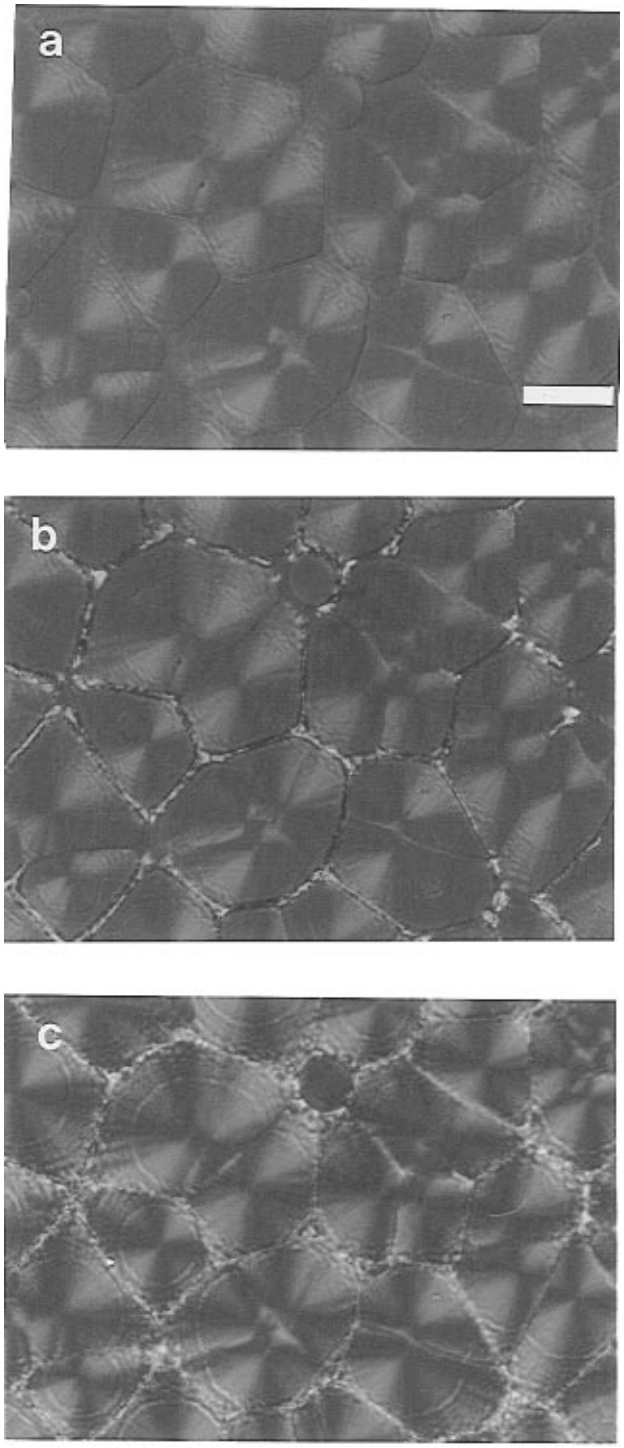

Figure 3. Crystallization of PBA from a 40/60 blend as observed by optical microscopy (same magnification, bar = 50 μm); (a) initial PVF_2 morphology at 150 °C; (b) development of PBA crystallites after 5 min at T_c = 40 °C; (c) completion of the crystallization of PBA after several hours at T_c = 40 °C. All micrographs correspond to the same section of the sample.

lization of PBA is observed within the spherulitic domains of the PVF_2 phase, i.e. in the interfibrillar channels of the PVF_2 spherulites. This is accompanied by a change in the birefringent appearance of the PVF_2 spherulites which are seen to become brighter and exhibit a more pronounced banding structure.

Figure 3 demonstrates that the formation of the semicrystalline/semicrystalline state is an intriguing process that is much more complicated than polymer crystallization from the homogeneous melt. It should be emphasized that the bulk crystallization of PBA

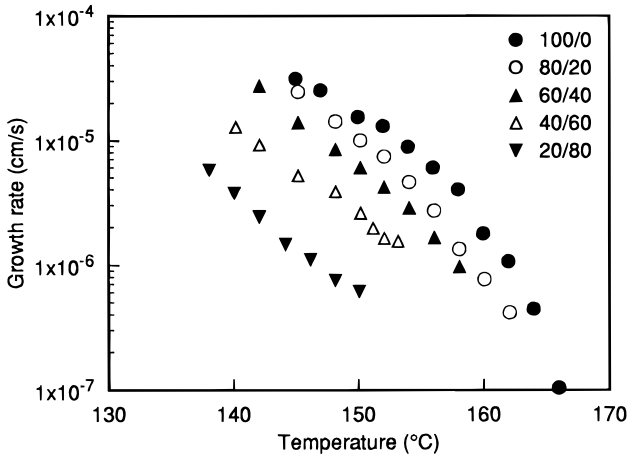

Figure 4. Radial spherulitic growth rate of PVF_2 as a function of T_c for various blend compositions.

proceeds through spherulitic growth with homogeneous nucleation. In the blends, however, nucleation appears to be heterogeneous and crystal growth according to a spherulitic morphology is not observed. The observation of extensive crystallization in the interspherulitic regions is of interest from the point of view of solid-state properties of semicrystalline polymers. Spherulitic boundaries are known to represent weak domains where crack propagation occurs with relative ease[22] and, therefore, modification of these grain boundaries using a second, crystalline polymer may lead to improvement of the mechanical behavior of the material.

Spherulitic Growth Rates of PVF_2. The radial growth rates (G) of PVF_2 spherulites in various blends containing up to 80 wt % PBA were determined by monitoring the spherulite radius R as a function of time during isothermal crystallization in the hot-stage of a polarizing microscope. For blends containing less than 60 wt % PBA, R was found to increase linearly in time up to the point of impingement, indicating a constant growth rate throughout the crystallization process. The linearity of R implies that PBA molecules, which are rejected from the growing PVF_2 crystals, do not migrate away from the spherulitic growth front, but rather become trapped within the interfibrillar regions of the growing spherulites.[15] In blends containing 60 wt % PBA or more, on the other hand, nonlinear growth of the spherulites was observed at the advanced stages of crystallization, indicating that in this case the noncrystalline material accumulates, to a certain extent, in the interspherulitic domains. These conclusions are consistent with microscopic observation, as shown in Figures 2 and 3.

Plots of the radial growth rate of PVF_2 spherulites as a function of the crystallization temperature (T_c) are shown in Figure 4 for different blend compositions. Measurement of growth rates is restricted to a certain temperature window limited by (a) a very high primary nucleation density at low temperatures and (b) very slow crystal growth and the formation of different crystal modifications at high temperatures. Since the available temperature windows are relatively small, no attempt is made to analyze the growth rate data in terms of the Hoffman−Lauritzen theory[23] of bulk polymer crystallization. In general, the Hoffman−Lauritzen model can be utilized to determine the kinetic parameters of the crystallization process. In order to do so in a meaningful way, growth rates must be known over a substantial portion of the growth rate curve,[3,24,25] and

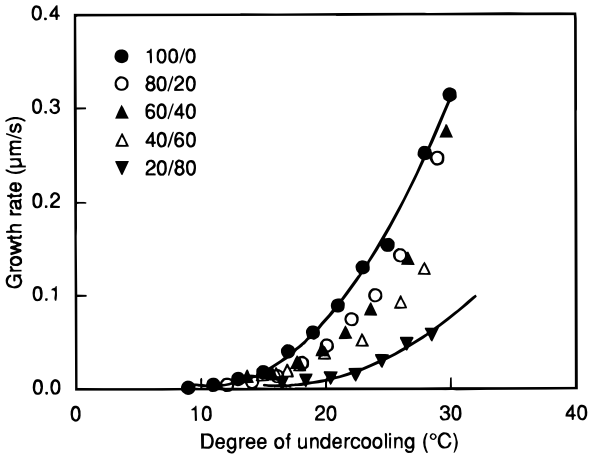

Figure 5. Spherulitic growth rates of PVF_2 as a function of the degree of undercooling for blends of various compositions.

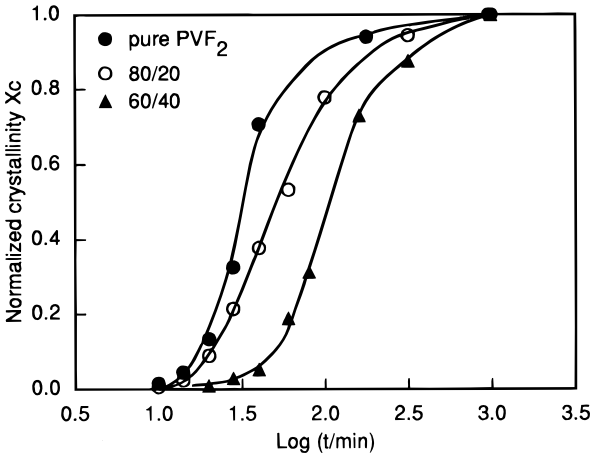

Figure 6. Crystallization isotherms for PVF_2 (T_c = 155 °C) at various blend compositions.

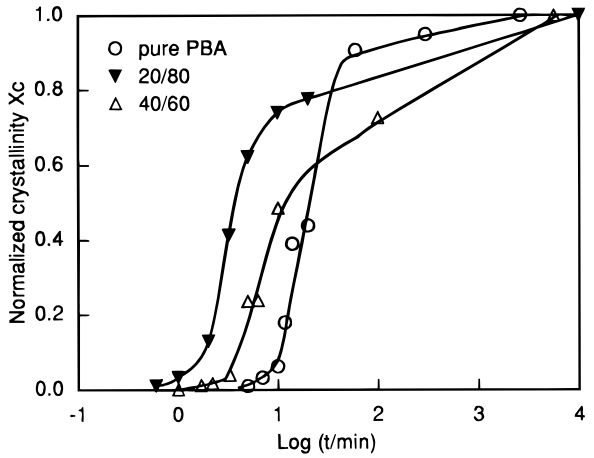

Figure 7. Crystallization isotherms for PBA (T_c = 43 °C) at various blend compositions.

this is clearly not the case in the present work. From the data shown in Figure 4, however, it is evident that the crystal growth rate of PVF_2 is depressed due to the addition of PBA. The growth rate reduction at a given T_c amounts to a factor of ~2.5 in blends containing 40 wt % PBA, and to a factor of ~25 when the PBA content reaches 80 wt %. It should be pointed out that this growth rate reduction is not related to changes in fluidity of the melt that may be of importance in blend systems showing a wide variation of T_g with blend composition.[3] In blends of PVF_2 and PBA, the variation of T_g with composition is small, especially when compared to the width of the $T_m - T_g$ interval (see Figure 1). The observed crystallization rate depression, therefore, arises from either (a) a reduction of the driving force for crystallization due to changes in the equilibrium melting point[23,24] or (b) a dilution effect[26] associated with a diminished concentration of crystallizable elements at the crystal growth front. In order to assess the effects of melting point depression on the crystal growth rate, we have plotted G as a function of the degree of supercooling ΔT for different blend compositions in Figure 5. It is seen that the growth rate data do not show a unique dependence on ΔT and that, at a given ΔT, the crystal growth rate is lower for the blends than it is for the pure polymer. Thus, the observed rate reduction cannot be attributed to changes in the equilibrium melting point alone. It is therefore reasonable to assume that the observed reduction of the crystal growth rate of PVF_2 in its blends with PBA is a result of the combined effects of melting point depression and dilution produced by the presence of the noncrystallizable PBA component.

As shown in Figures 2 and 3, samples of PVF_2/PBA blends, in the amorphous/semicrystalline state, are completely filled with more or less impinged spherulites, as a result of which PBA is not capable of crystallization with a spherulitic morphology. Thus, the kinetics of PBA crystallization cannot be followed by measurement of spherulitic growth rates. For this reason, we have further characterized the crystallization kinetics in PVF_2/PBA blends through determination of the overall crystallization rates of both PVF_2 and PBA using differential scanning calorimetry.

Overall Crystallization Rates. The overall crystallization kinetics in blends of PVF_2 and PBA were studied by following the change in crystallinity with time during the isothermal crystallization of different blends at either 155 °C (crystallization of PVF_2) or 43 °C (crystallization of PBA). The results of these experiments are expressed in terms of the "normalized crystallinity" $X(t)$, which is defined as the ratio of the heat of fusion after a certain crystallization time $\Delta H(t)$, to the heat of fusion after complete crystallization ΔH_∞, i.e., $X(t) = \Delta H(t)/\Delta H_\infty$. This quantity does not represent the real crystallinity, since ΔH_∞ does not correspond to the heat of fusion of 100% crystalline material, but it is a useful measure of how far the process of crystallization has advanced.

Typical crystallization isotherms for PVF_2, in the bulk and in the 80/20 and 60/40 blends, are shown in Figure 6. The isotherms show a progressive shift toward longer crystallization times as the amount of PBA in the blends increases, indicating that the overall crystallization kinetics of PVF_2 are slowed down as a result of blending. This is in qualitative agreement with the reduction of spherulitic growth rates of PVF_2 upon addition of PBA, as assessed by microscopy (Figure 4). The crystallization isotherms for PBA, in the bulk and in different blends, are shown in Figure 7. Of immediate interest is the fact that the isotherms for the blends are shifted toward shorter crystallization times with respect to pure PBA, implying that the overall crystallization of PBA in the blends is faster than it is in the pure polymer. It is seen that the overall crystallization is fastest in the 20/80 blend, which means that the crystallization rate goes through a maximum when plotted as a function of PVF_2 content. In order to illustrate this, the overall crystallization rate, which is defined as the reciprocal

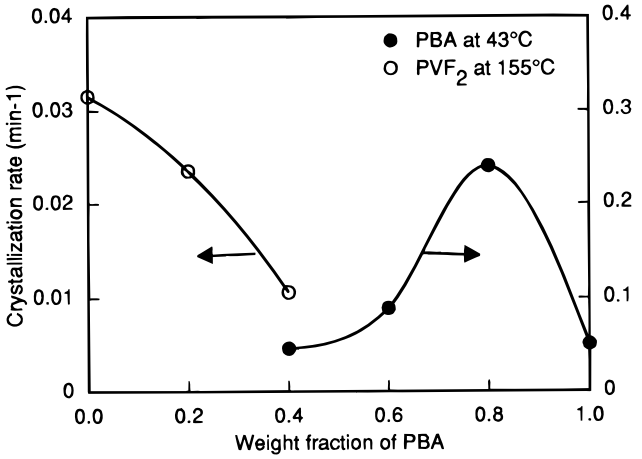

Figure 8. Overall crystallization rate vs blend composition for (○) PVF_2 at $T_c = 155$ °C and (●) PBA at $T_c = 43$ °C.

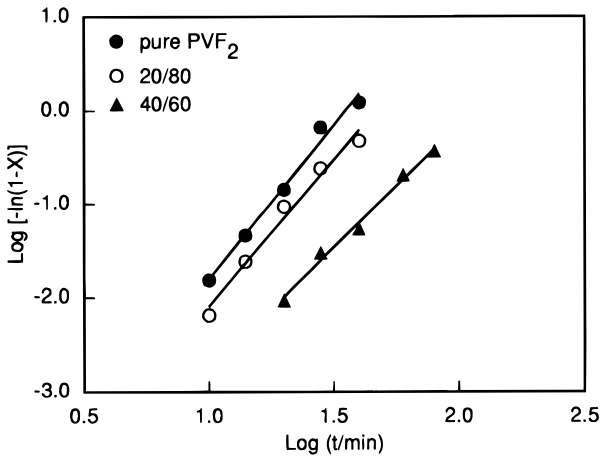

Figure 9. Avrami plots for PVF_2 at $T_c = 155$ °C at various blend compositions.

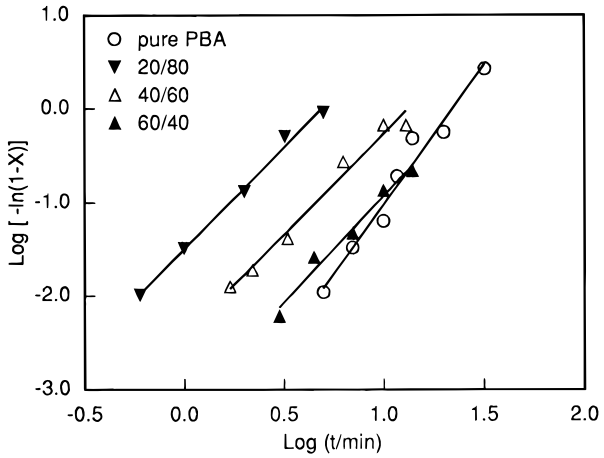

Figure 10. Avrami plots for PBA at $T_c = 43$ °C at various blend compositions.

value of the time required to achieve 50% of the final crystallinity of the sample, is plotted as a function of blend composition in Figure 8. It can be seen that for PVF_2, the overall crystallization rate decreases monotonically with blend composition, whereas in the case of PBA, it exhibits a distinct maximum. In blends containing 20 wt % PVF_2, the overall crystallization is approximately 5 times faster than it is for pure PBA. A further increase of the PVF_2 concentration results in a subsequent decrease of the overall crystallization rate.

It is conceivable that the remarkable dependence of the overall crystallization rate of PBA on blend composition is associated with the fact that the PVF_2 phase is always partially solidified at temperatures where crystallization of PBA occurs. It was mentioned earlier that the bulk crystallization of PBA proceeds with homogeneous nucleation. In the blends, on the other hand, the solid PVF_2 phase provides a foreign surface where heterogeneous nucleation can take place, which is expected to lead to much higher nucleation rates for PBA. Such an increased nucleation rate was indeed observed by microscopy (Figure 3) and offers a plausible explanation for the initial increase in the overall crystallization rate upon addition of PVF_2. A similar phenomenon has been observed in incompatible blends of poly(ethylene terephthalate) (PET) and polyamide-6,6 (PA), where heterogeneous nucleation due to the presence of PA was found to prevent the possibility of supercooling of PET into a fully amorphous state.[27] The addition of PVF_2 will result not only in an increase of nucleation rate but also in a decrease of the linear growth rate of the PBA crystals due to a dilution effect which reduces the number of crystallizable units at the crystal growth front. This effect becomes more important as the concentration of PVF_2 in the blends increases and will reduce the overall crystallization rate of PBA as the blends become richer in PVF_2. Thus, the maximum in the overall crystallization rate of PBA vs blend composition most likely arises from a combined effect of enhanced nucleation and slower crystal growth rates.

The crystallization isotherms shown in Figures 6 and 7 exhibit the familiar sigmoidal shape and may be analyzed in terms of the well-known Avrami equation[28]

$$1 - X = \exp(-kt^n) \tag{1}$$

where X is the normalized crystallinity, k is a rate constant and n is the Avrami exponent which denotes the nature of the nucleation and growth process. Equation 1 may be rewritten as

$$\log[-\ln(1 - X)] = \log k + n \log t \tag{2}$$

A plot of the left-hand side of (2) vs log t should yield a straight line from which the Avrami exponent can be determined. This procedure is illustrated in Figures 9 and 10 for the isothermal crystallization data of PVF_2 and PBA, respectively, and the results are summarized in Table 1. From the Avrami analysis it emerges that the crystallization of PVF_2, in the pure state as well as in the blends, is characterized by $n = 3$. Thus, although the overall crystallization rate decreases, the nucleation

Table 1. Crystallization Data for PVF_2/PBA Blends

crystallization of PVF_2 at 155 °C			crystallization of PBA at 43 °C		
blend	overall crystallization rate (min^{-1})	Avrami exponent, n	blend	overall crystallization rate (min^{-1})	Avrami exponent, n
100/0	0.032	3.3	0/100	0.051	3.0
80/20	0.023	3.1	20/80	0.240	2.1
60/40	0.011	2.8	40/60	0.089	2.1
			60/40	0.040	2.2

mechanism and geometry of crystal growth of the PVF_2 phase is not affected by the presence of PBA. The value of $n = 3$ suggests that the crystallization of PVF_2 proceeds via three-dimensional growth with athermal nucleation,[29] which is consistent with microscopic observation of the crystallization process.

Similar to the case of PVF_2, the free crystallization of pure PBA is characterized by a value of the Avrami exponent of $n = 3$. However, the crystallization of PBA in the blends appears to be governed by $n = 2$, indicating that, in the blended state, the crystallization of PBA adheres to a different mechanism of nucleation and/or growth. This finding is supported by microscopic observation (Figure 3) which has shown that crystallization of PBA in the blends is substantially different from the simple spherulitic growth mechanism in the undiluted polymer. Although the exact meaning of n is not entirely clear in the present case, the decrease in n upon the addition of PVF_2 reflects a decrease in the number of dimensions in which crystal growth can take place.[29] This is consistent with the fact that crystallization of PBA is physically constrained by the spherulitic microstructure of the PVF_2 phase.

These results emphasize that the crystallization of PBA is profoundly influenced by the presence of PVF_2. The most important effects are a drastic change in crystalline morphology, a pronounced increase in the overall crystallization rate with small amounts of PVF_2, and a change in the Avrami exponent. These effects appear to be inter-related and can all be attributed to the fact that the PVF_2 phase is partially solidified at the temperatures where PBA crystallization takes place and, in this way, affects the nucleation, growth, and morphology of this low-T_m component.

Conclusions

In miscible blends of PVF_2 and PBA, both components are capable of crystallization over a wide range of compositions. Since the two polymers crystallize in well-separated temperature regimes, and are structurally dissimilar, cocrystallization does not occur. Thus, the crystallization of each of the two blend components represents a phase separation process in which the polymers partially segregate from the mixture to form a pure phase. The present investigation of the kinetics of these crystallization processes and of the resultant crystalline morphologies has revealed that each component affects the crystallization behavior of the other in a variety of ways. During the crystallization of the high-T_m component (PVF_2), the second component acts as a noncrystalline diluent which reduces the spherulitic growth rate as well as the overall crystallization rate of the PVF_2 phase. Furthermore, the addition of PBA affects the spherulitic texture of the PVF_2 phase and facilitates formation of the PVF_2 γ-polymorph. Since PBA is noncrystalline at the temperatures at which PVF_2 crystallizes, these effects are not strictly pertinent to the semicrystalline/semicrystalline nature of this blend system and have been observed in blends of PVF_2 with amorphous polymers. On the other hand, crystallization of the low-T_m component (PBA) represents the transition from the amorphous/semicrystalline to the semicrystalline/semicrystalline state and is in this sense unique to blends composed of two crystalline polymers. The crystallization of PBA appears to be strongly influenced by the presence of PVF_2, which can be attributed to the fact that the PVF_2 phase is partially solidified at the temperatures where PBA crystallization takes place. The overall crystallization rate of PBA goes through a maximum when plotted as a function of PVF_2 content, due to the combined effects of enhanced nucleation and slower crystal growth rates. The mechanisms of nucleation and crystal growth of the PBA phase are profoundly modified in the presence of PVF_2, as observed by optical microscopy and reflected in a change of the Avrami exponent. Crystallization of the PBA phase initially takes place in the interspherulitic domains of the PVF_2 microstructure, while at the advanced stages, crystallization of PBA in the interfibrillar pockets of the PVF_2 spherulites is also evident. The extensive crystallization of the low-T_m component at the spherulite boundaries could be of importance with respect to the improvement of mechanical properties of semicrystalline polymers in general.

Acknowledgment. This work has been supported through an operating grant from the Natural Sciences and Engineering Research Council of Canada (NSERC).

References and Notes

(1) Robeson, L. M. *J. Appl. Polym. Sci.* **1973**, *17*, 3607.
(2) Nishi, T.; Wang, T. T. *Macromolecules* **1975**, *8*, 909.
(3) Wang, T. T.; Nishi, T. *Macromolecules* **1977**, *10*, 421.
(4) Ong, C. J.; Price, F. P. *J. Polym. Sci., Polym. Symp.* **1978**, *63*, 59.
(5) Morra, B. S.; Stein, R. S. *J. Polym. Sci., Polym. Phys. Ed.* **1982**, *20*, 2261.
(6) Martuscelli, E. *Polym. Eng. Sci.* **1984**, *24*, 563.
(7) Cheung, Y. W.; Stein, R. S.; Wignall, G. D.; Yang, H. E. *Macromolecules* **1993**, *26*, 5365.
(8) Cheung, Y. W.; Stein, R. S. *Macromolecules* **1994**, *27*, 2512.
(9) Cheung, Y. W.; Stein, R. S.; Lin, J. S.; Wignall, G. D. *Macromolecules* **1994**, *27*, 2520.
(10) Cheung, Y. W.; Stein, R. S.; Chu, B.; Wu, G. *Macromolecules* **1994**, *27*, 3589.
(11) Penning, J. P.; Manley, R. St. J. *Macromolecules* **1996**, *29*, 77.
(12) Keith, H. D.; Padden, F. J., Jr.; Russell, T. P. *Macromolecules* **1989**, *22*, 666.
(13) Pizzoli, M.; Scandola, M.; Cerrorulli, G. *Macromolecules* **1994**, *27*, 4755.
(14) Keith, H. D.; Padden, F. J., Jr. *J. Appl. Phys.* **1964**, *35*, 1270.
(15) Keith, H. D.; Padden, F. J., Jr. *J. Appl. Phys.* **1964**, *35*, 1286.
(16) Lovinger, A. J. *J. Polym. Sci., Polym. Phys. Ed.* **1980**, *18*, 793.
(17) Prest, W. M., Jr.; Luca, D. J. *J. Appl. Phys.* **1975**, *46*, 4136.
(18) Lovinger, A. J.; Keith, H. D. *Macromolecules* **1979**, *12*, 919.
(19) Weinhold, S.; Litt, M. H.; Lando, J. B. *J. Polym. Sci., Polym. Lett.* **1979**, *17*, 585.
(20) Morra, B. S.; Stein, R. S. *J. Polym. Sci., Polym. Phys. Ed.* **1982**, *20*, 2243.
(21) Braun, D.; Jacobs, M.; Hellmann, G. P. *Polymer* **1994**, *35*, 706.
(22) Friedrich, K. *Prog. Colloid Polym. Sci.* **1978**, *64*, 103.
(23) Hoffman, J. D.; Lauritzen, J. I., Jr. *J. Res. Natl. Bur. Stand., Sect. A* **1961**, *65*, 297.
(24) Hoffman, J. D.; Davis, G. T.; Lauritzen, J. I., Jr. In *Treatise on Solid State Chemistry*; Hannay, N. B., Ed.; Plenum: New York, 1976; Vol. 3.
(25) Lovinger, A. J.; Davis, D. D.; Padden, F. J., Jr. *Polymer* **1985**, *26*, 1595.
(26) Boon, J.; Azcue, J. M. *J. Polym. Sci., Polym. Phys. Ed.* **1968**, *6*, 885.
(27) Kamal, M. R.; Sahto, M. A.; Utracki, L. A. *Polym. Eng. Sci.* **1982**, *22*, 1127.
(28) Avrami, M. *J. Chem. Phys.* **1941**, *9*, 177.
(29) Wunderlich, B. *Macromolecular Physics*; Academic Press: New York, 1976; Vol. 2.

MA950652L